34th Annual International Conference of the IEEE EMBS
San Diego, California USA, 28 August - 1 September, 2012

Comprehensive characterization of tungsten microwires in chronic neurocortical implants

Abhishek Prasad, *Member IEEE,* Qing-Shan Xue, Viswanath Sankar, *Member IEEE*, Toshikazu Nishida, *Senior Member IEEE*, Gerry Shaw, Wolfgang Streit, and Justin C. Sanchez, *Member IEEE*

***Abstract* — The long-term performance of chronic microelectrode array implants for neural ensemble recording is affected by temporal degradation in signal quality due to several factors including structural changes in the recording surface, electrical responses, and tissue immune reactivity. This study combines the information available from the temporal aggregation of both biotic and abiotic metrics to analyze and quantify the combined effects on long-term performance. Study of a 42-day implant showed there was a functional relationship between the measured impedance and the array neuronal yield. This was correlated with structural changes in the recording sites, microglial activation/degeneration, and elevation of a blood biochemical marker for axonal injury. We seek to elucidate the mechanisms of chronic microelectrode array failure through the study of the combined effects of these biotic and abiotic factors.**

I. Introduction

There are over 2 million individuals in the U.S. alone suffering from various neurological disorders [1-3] who can greatly benefit from rehabilitative neuroprosthetics developed for activities of daily living. However, such assistive technology requires sampling of reliable neural signals for the entire duration that they are interfaced with neural tissue. The development of high-density microelectrode probes [4-6] has enabled the recording of signals from large neuronal ensembles however the current systems have been unable to access such signals for more than several years [5]. Ideally, such a neural interface system should be able to record reliable signals from the neuronal ensembles for the lifetime of the subject. Currently there are international efforts ongoing to understand the mechanisms of events that occur in the lifetime of chronic microelectrode arrays [7-20]. The goal is to identify the major failure modes that affect the implanted microelectrodes temporal degradation of array yield, signal-to-noise, and neuronal yield, ultimately resulting in electrode failure. Recording site deterioration can occur due to interplay of both biotic (tissue response, disruption of blood-brain barrier, astrocytic and microglial activation, etc.) [7-13] and abiotic factors (recording site changes post-implantation, corrosion, insulation damage, etc.) [14-15]. Current research has focused primarily single modes of failure following chronic microelectrode implantation [9-13, 16-18]. The unique part of this work is that it combines data from both the biotic and abiotic perspectives in a high resolution manner to study the changes occurring at the electrode-tissue interface that could provide insights into chronic electrode failure modes.

Manuscript received March 15, 2012. This work was sponsored by the Defense Advanced Research Projects Agency (DARPA) Microsystems Technology Office under the auspices of Dr. Jack Judy (jack.judy@darpa.mil) through the Space and Naval Warfare Systems Center, Pacific Grant No. N66001-11-1-4009.

J. C. Sanchez and A. Prasad are with the Department of Biomedical Engineering and the Miami Project to Cure Paralysis, University of Miami, Coral Gables, FL 33146, USA (phone: 305-243-4930 e-mail: a.prasad@miami.edu).

T. Nishida and V. Sankar are with the Department of Electrical and Computer Engineering, University of Florida, Gainesville, FL 32611, USA

W. Streit, Q-S Xue, and G. Shaw are with the Department of Neuroscience, University of Florida, Gainesville, FL 32611, USA.

G. Shaw is also CEO of EnCor Biotechnology Inc., Gainesville, FL 32608 USA.

II. Methods & Results

The experimental design discussed in this paper allowed for a comprehensive analysis of both biotic and abiotic metrics of tungsten microwire arrays implanted into the rat somatosensory cortex. The animals were staggered in their implant durations according to the various phases reported in the literature namely the acute [19], recovery [13], and chronic [8] periods associated with the lifetime of individual probes. Data from a 42-day implant period animal is presented throughout this paper.

A. Implant Procedure

All procedures were approved by the Institutional Animal Care and Use Community, University of Miami. Briefly, 16-channel microwire arrays (Tucker Davis Technologies, FL) consisting of polyimide insulated 50µm diameter tungsten microwires were implanted into the right hemisphere of the somatosensory cortex. A micropositioner (Kopf Instruments, CA) was used to drive the electrode array into the cortex and electrophysiologic recordings were performed simultaneously to locate the layer V pyramidal neurons (approximately 1.6mm from the cortical surface). Dental cement (A-M Systems) attached to four skull screws was used to hold the electrode array and the microconnector in place. One skull screw posterior to the electrode array served as the common ground and was connected via a stainless steel wire.

B. Electrode Array Imaging

All tungsten microwire arrays were imaged prior to implantation and post-explantation using a scanning electron microscope (CarryScope SEM, JEOL, Inc. and FEI XL-40 field emission gun SEM). SEM imaging provided a basis for comparing the structural changes that occurred following chronic implantation of these arrays for varying lengths of implant duration. Figure 1 (left panel) shows a SEM image of four representative electrodes taken prior to implantation. Figure 1 (right panel) shows the structural changes on the same four electrodes (wires) 42-days post-implantation in the animal. Note the flat recording surfaces at the electrode tips in left panel are replaced by corroded surfaces in the right panel. The black mark on one of the electrodes in the left panel was due to the laser-cutting method used by the

manufacturer. Post-implant electrode recording sites presented with concave indentations in the surface. Insulation damage at the recording sites can also be observed in the right panel. The material on two wires in the right panel is the carbon paint used to coat the sample before loading into the SEM.

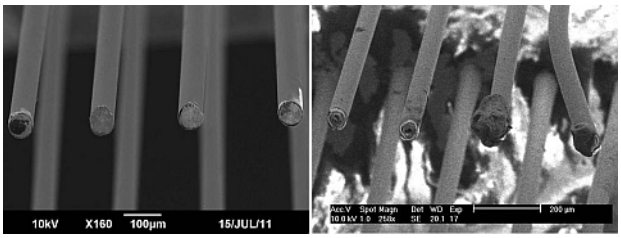

Figure 1. Pre-implant and post-explant SEM images of the same electrodes show the structural changes on the recording sites.

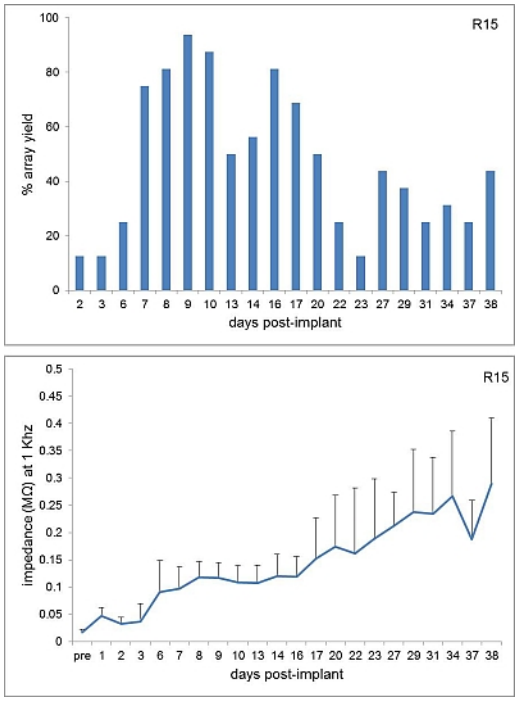

Figure 2. Temporal variation of the array yield (top) and the average impedance (bottom) for a 42-day implant period.

C. Electrode Impedance Spectroscopy

Daily impedance measurements were performed *in vivo* using a NanoZ impedance tester (TDT, FL). The impedances of the tungsten microwires were measured with respect to a distant low impedance stainless steel reference wire tied to a skull screw. Impedances were measured *in vitro* in saline prior to implantation and then *in vivo* in freely moving awake animals before each of the recording sessions. 1KHz frequency was used as the choice of frequency to report results as it is the fundamental frequency for an action potential [19].

D. Electrophysiological Recording and Data Analysis

Neural recordings were performed using a real-time signal processing and storage system (RZ2, TDT, FL). Raw neural signals were acquired at 24414.06Hz and then band-pass filtered between 0.5-6KHz. Filtered signals were spike

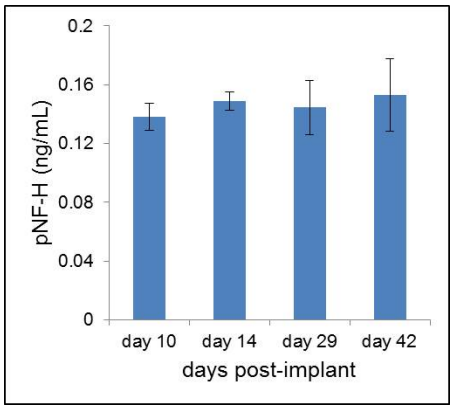

Figure 3. Blood pNF-H levels indicating elevated levels of the axonal injury biomarker during the 42-day implant duration. Data is normalized against control rat blood, which does not contain pNF-H.

sorted online during data collection as well as offline using OpenSorter (TDT, FL). The functional property of the electrode array reported here was quantified by the array yield which was defined as the fraction of electrodes that were able to isolate at least a single neuron. Larger array yields are desirable as they correspond to more functioning electrodes in each electrode array. Fig. 2 (top) shows the array yield for recordings up to day 38 for a 42-day implant period. The yield was observed to be low following surgery up to the 1-week mark that can be attributed to trauma following electrode implantation. The average electrode impedance was also low (bottom panel) during this time. The impedance increased 1.5-2 times at the 1-week period which corresponded with an increase in array yield. As the implant progressed to a chronic period, the array yield dropped by the three-week mark and then remained around this value for the remainder of the implant period. Overall, there was a functional relationship between the array yield and the measured impedance. The microwire array showed progressive increases in impedance during the 42-day implant period (Fig. 2). Interestingly, by day 6 the impedance increased to 100 KΩ and remained relatively flat up to day 16. During this time the best neuronal yield was obtained. We observed that the array yield tended to be low when the average impedance was below 40KΩ. However, as the impedance continued to increase beyond 150KΩ (days 17+ in Fig. 2), a decrease in yield was observed. In general, the best yields were obtained when the impedance of these tungsten microwires fell within the 40-150KΩ range.

E. Serum Sampling and Analysis

Blood samples (0.5mL each time) were collected at regular intervals using a tail vein-puncture from the animals. 20µL of the serum was run on ELISA assays for pNF-H using procedures outlined in detail elsewhere [21]. pNF-H, a heavily phosphorylated axonal form of the neurofilament subunit NF-H has been reported as a novel blood biomarker for axonal injury [21]. The presence of this biomarker in the blood indicates that damage or degeneration of axons is underway and it is not present in uninjured animals. Continuous monitoring of the biomarker at regular intervals can provide peripheral insight into the brain injury caused by

the implant. A sustained elevation indicates ongoing damage occurring in the neuronal environment around the implanted devices. Figure 3 shows elevated blood levels of the pNF-H biomarker on days 10, 14, 29, and 42 in the animal. These results suggest that there was a chronic injury response occurring in the microenvironment surrounding the implant causing the persistent release of this biomarker. We are measuring the release of this protein into blood longitudinally as a potential means of predicting electrode failure. It is significant that this biomarker can be readily detected in blood as this suggests that comparable analysis of patients with electrode implants will be feasible. Blood is of course much more readily and routinely obtained from patients than CSF, another potential source of CNS injury biomarkers.

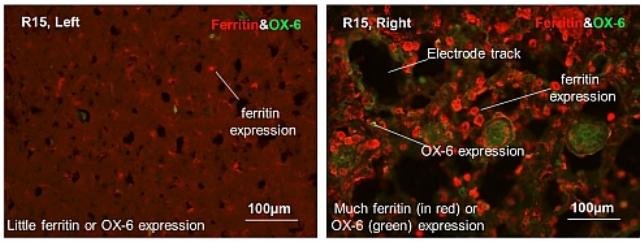

Figure 4. Histopathology of control (left) vs implanted (right) tissue.

F. Histology

Animals were transcardially perfused with 10% formalin solution as the fixative. The electrode array was gently removed from the cortical tissue and the tissue was then cryoprotected using 30% sucrose in phosphate-buffered saline. 20µm thick frozen sections were then cut on a cryostat. The ferritin and OX-6 expression in the tissue harboring the electrode array in relation to surrounding microglial cells was examined using double fluorescent immunolabeling as described elsewhere [20] (Fig. 4). Both OX-6 and ferritin expression are increased following injury during microglial activation. While mechanisms of increased OX-6 expression are likely related to generally enhanced immunological readiness of microglia during activation, increased expression of ferritin on microglia probably occurs for different reasons and affects a different and larger microglial subpopulation. Since ferritin is used by cells to sequester free iron atoms (both ferric and ferrous), its upregulation likely signifies an attempt by microglia to take up and store iron entering into the CNS parenchyma through a compromised blood-brain barrier. The left panel in Fig. 4 shows an image from cortical tissue in the left (unimplanted) somatosensory cortex where there is only minimal expression of ferritin and no OX-6 expression. The right panel shows increased expression of both the antigens in the right (implanted) cortex close to the electrode array. These findings, together with our abiotic, electrophysiological, and biochemical data, all point towards a chronic and persistent brain injury that is marked perhaps most significantly by a permanently disrupted blood brain barrier, which in essence could account for all of the derangements described (i.e. electrode corrosion, elevated serum levels of brain proteins, loss of neuronal yield and gradually increasing impedance, chronic neuroinflammation and overexpression of iron-sequestering protein).

III. Conclusions

This study aimed at understanding the mechanisms involved in the chronic electrode implantation by combining both biotic and abiotic functional metrics. These functional metrics can be quantified and may be used to provide predictions that could improve future electrode performance. The results from this study show that electrode failure or a decrease in performance is due to interplay of both biotic and abiotic factors. Controlling one or more of these factors and providing interventions may improve long-term electrode performance.

References

[1] D. L. Brown-Triolo, M. J. Roach, K. Nelson, and R. J. Triolo, "Consumer perspectives on mobility: Implications for neuroprosthesis design," *Journal of Rehabilitation Research and Development,* vol. 39, pp. 659-669, 2002.

[2] C. Sadowsky, O. Volshteyn, L. Schultz, and J. W. McDonald, "Spinal Cord Injury," *Disability and Rehabilitation* vol. 24, pp. 680-687, 2002.

[3] H. Hirschfeld, "Motor control of every day motor tasks: Guidance for neurological rehabilitation," *Physiology and Behavior,* vol. 92, pp. 161-166, 2007.

[4] P. J. Rousche and R. A. Normann, "Chronic recording capability of the utah intracortical electrode array in cat sensory cortex," *Journal of Neuroscience Methods,* vol. 82, pp. 1-15, 1998.

[5] J. D. Simeral, S. P. Kim, M. J. Black, J. P. Donoghue, and L. R. Hochberg, "Neural control of cursor trajectory and click by a human with tetraplegia 1000 days after implant of an intracortical microelectrode array," *Journal of neural engineering,* vol. 8, 2011.

[6] S. Musallam, M. J. Bak, P. R. Troyk, and R. A. Andersen, "A floating metal microelectrode array for chronic implantation," *J Neurosci Methods,* vol. 160, pp. 122-7, Feb 15 2007.

[7] J. Thelin, H. Jörntell, E. Psouni, M. Garwicz, J. Schouenborg, N. Danielsen, and C. E. Linsmeier, "Implant size and fixation mode strongly influence tissue reactions in the CNS," *PLoS ONE,* vol. 6, 2011.

[8] G. C. McConnell, H. D. Rees, A. I. Levey, C. A. Gutekunst, R. E. Gross, and R. V. Bellamkonda, "Implanted neural electrodes cause chronic, local inflammation that is correlated with local neurodegeneration," *Journal of neural engineering,* vol. 6, 2009.

[9] D. H. Szarowski, M. D. Andersen, S. Retterer, A. J. Spence, M. Isaacson, H. G. Craighead, J. N. Turner, and W. Shain, "Brain responses to micro-machined silicon devices," *Brain Research,* vol. 983, pp. 23-35, 2003.

[10] J. N. Turner, W. Shain, D. H. Szarowski, M. Andersen, S. Martins, M. Isaacson, and H. Craighead, "Cerebral astrocyte response to micromachined silicon implants," *Experimental Neurology,* vol. 156, pp. 33-49, 1999.

[11] D. J. Edell, T. Vo Van, V. M. McNeil, and L. D. Clark, "Factors influencing the biocompatibility of insertable silicon microshafts in cerebral cortex," *IEEE Transactions on Biomedical Engineering,* vol. 39, pp. 635-643, 1992.

[12] H. Lee, R. V. Bellamkonda, W. Sun, and M. E. Levenston, "Biomechanical analysis of silicon microelectrode-induced strain in the brain," *Journal of neural engineering,* vol. 2, pp. 81-89, 2005.

[13] B. D. Winslow and P. A. Tresco, "Quantitative analysis of the tissue response to chronically implanted microwire electrodes in rat cortex," *Biomaterials,* vol. 31, pp. 1558-1567, 2010.

[14] J. C. Sanchez, N. Alba, T. Nishida, C. Batich, and P. R. Carney, "Structural modifications in chronic microwire electrodes for cortical neuroprosthetics: A case study," *IEEE Transactions on Neural Systems and Rehabilitation Engineering,* vol. 14, pp. 217-221, 2006.

[15] E. Patrick, M. E. Orazem, J. C. Sanchez, and T. Nishida, "Corrosion of tungsten microelectrodes used in neural recording applications," *Journal of Neuroscience Methods,* vol. 198, pp. 158-171, 2011.

[16] J. C. Williams, J. A. Hippensteel, J. Dilgen, W. Shain, and D. R. Kipke, "Complex impedance spectroscopy for monitoring tissue responses to inserted neural implants," *Journal of neural engineering,* vol. 4, pp. 410-423, 2007.

[17] J. C. Williams, R. L. Rennaker, and D. R. Kipke, "Stability of chronic multichannel neural recordings: Implications for a long-term neural interface," *Neurocomputing,* vol. 26-27, pp. 1069-1076, 1999.

[18] J. P. Frampton, M. R. Hynd, M. L. Shuler, and W. Shain, "Effects of glial cells on electrode impedance recorded from neuralprosthetic devices in vitro," *Ann Biomed Eng.,* vol. 38, pp. 1031-47, 2010.

[19] M. P. Ward, P. Rajdev, C. Ellison, and P. P. Irazoqui, "Toward a comparison of microelectrodes for acute and chronic recordings," *Brain Research,* vol. 1282, pp. 183-200, 2009.

[20] A. Prasad, V. Sankar, A. T. Dyer, E. Knott, Q.-S. Xue, T. Nishida, J. R. Reynolds, G. Shaw, W. Streit, and J. C. Sanchez, "Coupling Biotic and Abiotic Metrics to Create a Testbed for Predicting Neural Electrode Performance," *Conf Proc IEEE Eng Med Biol Soc*, vol. 2011, pp. 3020-3, 2011.

[21] G. Shaw, C. Yang, R. Ellis, K. Anderson, J. P. Mickle, S. Scheff, B. Pike, D. K. Anderson, and D. Howland," Hyperphosphorylated neurofilament NF-H is a serum biomarker of axonal injury," *Biochem Biophys Res Comm.* vol. 336, pp. 1268-1277, 2005.